Electronic Supplementary Material (ESI) for Journal of Materials Chemistry A

Modifying the cellular properties via rational chemical design for unnatural oxygen reduction electrocatalysis of a cell

Yangdi Niu, Gaofu Guo, Deming Xue, Xiaoli Yang, Xianqi Dai*, Zhengyu Bai*, Lin Yang*

Collaborative Innovation Center of Henan Province for Green Manufacturing of Fine Chemicals; Key Laboratory of Green Chemical Media and Reactions, Ministry of Education, School of Chemistry and Chemical Engineering, College of Life Sciences, College of Physics, Henan Normal University, Xinxiang, Henan 453007, P. R. China.

E-mail: yanglin@htu.edu.cn; baizhengyu@htu.edu.cn; xqdai@htu.edu.cn

Experimental section

Bacteria culture

The preserved *Escherichia coli* (*E. coli*) BL-21 strains were first resuscitated and rejuvenated in 5 ml of LB medium. The bacteria solution was put in a 37 ℃ shaker for at least 12 h (usually overnight). Subsequently, 200 μL of bacteria colonies were taken out and put in another flask containing 200 ml of fresh LB solution for further growth. When the final bacteria solution's OD_{600} is about 1.5, the cells were harvested by centrifugation (5000 rpm, 5 min) for further use.

Synthesis of *E. coli* cell@Fe-TA

The harvested *E. coli* cells were washed with ultrapure water for two times, and then suspended in 10 mL aqueous solution of tannic acid (TA, 2 mg mL^{-1}). The mixed bacteria solution is strongly swirled for one minute at room temperature to bind TA tightly to the cells. And then, 10 mL aqueous solution of iron (III) chloride (40 mg mL^{-1}) was added into the above solution rapidly and further swirled for one minute, making Fe(III) ions chelate with TA molecular. So, the *E. coli* cell@Fe-TA was obtained by the mentioned method.

Characterization of *E. coli* cell@Fe-TA

The surface morphology of native *E. coli* cell and *E. coli* cell@Fe-TA was characterized by scanning electron microscopy (SEM, Hitachi, SU8100, Japan). SEM test sample preparation procedure is as follows. After the fresh cell samples were cleared with PBS solution, they were immediately put into the electron microscope fixative (2.5% glutaraldehyde) at room temperature for 2 h, then were transferred to 4℃ condition and stored for 9 h. The obtained bacteria precipitates dehydrated with a series of concentration gradients of ethanol (30%, 50%, 70%, 80%, 90 % and 100%) for 15 minutes per time, respectively. Finally, the samples were dried and observe with SEM and SEM-EDS to obtain the images.

The interior morphology of native *E. coli* cell and *E. coli* cell@Fe-TA was characterized by transmission electron microscopy (TEM, Hitachi, HT7800, Japan). When undergoing the same immobilization and dehydration processes described above,

bacteria precipitate wrapped in the resin and polymerized in the oven at 60 ℃ for at least 48 h. After that, ultrathin sections of 70 nm were performed and deposited on the copper grids for imaging with TEM or HAADF-STEM-EDS.

The coordinated structure of Fe-TA complexes on *E. coli* cell was further characterized by various spectral measurements including X-ray photoelectron spectroscopy (XPS, Escalab 250Xi, Thermo Scientific, USA), UV/Vis absorption spectra (Cary 100 system), Raman spectrum (LabRAM HR Evolution, Manufactred at Villeneuve d'Ascq, France, Fourier transform infrared (FTIR) spectroscopy (IRTrAcer-100, Shimadzu, Japan) and ^{1}H NMR spectroscopy (AVANCE NEO 400MHZ) was tested with better water suppression by the two-time WATERSUP impulse train template method (pulprog: noesygppr1d).

Viability test

The cell viability detection kit containing two fluorescent dyes of NucGreen (green) and EthD-III (red) is used to evaluate the bacteria viability of native and engineered *E. coli* cell. 1 mL of bacteria solution cultured to an advanced stage of logarithmic growth were centrifuged (5000 rpm, 10 min), and the bacteria precipitate was then suspended by adding 1 ml of 0.85% sodium chloride solution. The prepared dyeing solution (1 μL NucGreen and 2 μL EthD-III mixed in 8 μL 0.85% sodium chloride solution) was added to the bacterial suspension and incubated at room temperature for 15 min away from light. The stained cells were detected by a Leica TCS SP8 confocal laser scanning microscope (CLSM, Germany).

Cell growth test

The cell-division ability of native and engineered *E. coli* cell was monitored by the growth test in LB medium. The cell optical density was tested according to the turbidity at 600 nm (OD_{600}) by the UV/Vis absorption spectra (Cary 100 system).

Binding detection of intracellular Cyt c and Fe-TA nanocomplexes

To demonstrate that intracellular Cyt c proteins can successfully bind to and interact with Fe-TA nanocomplexes, sodium dodecyl sulphate polyacrylamide gel electrophoresis (SDS-PAGE) was carried out. Firstly, the prepared *E. coli* cells@Fe-TA and control *E. coli* cells sample were ultrasonically broken and lysed, respectively, to

release the intracellular protein. Subsequently, the cell suspension was centrifuged so that the proteins were extracted into the supernatant solution. Ultimately, the supernatant was electrophoresed in 5% (w/v) concentrated gel for 20 min at 80 V, and in 12% (w/v) separating gel for 1 h at 120 V. The protein gel was stained by Coomassie Brilliant Blue R-250 and faded by destainer.

Construction of bioelectrode

The cell pellet obtained by centrifugation of 50 ml bacterial solution was suspended in 50 mL fresh LB medium, and then several pieces of carbon cloth purified with acetone, concentrated HCl and HNO_3 and ultrapure water were immersed into the cell suspension. Afterwards, the mixture was placed in a shaker (200 rpm) at 37 ℃ for 36 h to an ultimate optical density of OD_{600} = 2.65. So that, the *E. coli* cells were firmly attached on the carbon cloth in the way of natural growth.

Electrochemical analyses

The ORR performance measurements were conducted on a CHI 760E electrochemical workstation (Shanghai Chenhua, China) with a typical three-electrode configuration using a carbon cloth (CC) electrode (1×1cm) as the working electrode and a platinum (Pt) sheet and saturated silver-silver chloride (Ag/AgCl) electrode as the counter and reference electrode, respectively. Through a series of concetration optimization of TA and Fe^{3+}, electrochemical measurements were performed in 80 mL M9 buffer (PH 7) composed of 22 mM KH_2PO_4, 42 mM Na_2HPO_4, 85.5 mM NaCl, 1.0 mM $MgSO_4$ and 0.1 mM CaCl2 at a temperature of 37℃. Cyclic voltammetric (CV) measurements were performed after N_2 and O_2 saturated for 30 minutes with a scanning speed of 50 mV s^{-1}. Linear sweep voltammetry (LSV) curves were obtained in O_2 saturated M9 buffer with a scanning speed of 5 mV s^{-1}. Electrochemical impedance spectroscopy (EIS) analysis was carried out at a potential of -0.3 V.

MFC device setup

Classical H-type dual-chamber MFC with internal working volume of 50 ml separated by a proton exchange membrane (nafion 211, DuPont) was employed in this study. Carbon cloth (CC, 2×2cm) were used as the electrodes for cathode and anode. The electrolyte of cathodic chamber was M9 buffer solution containing 4 g/L glucose

as the carbon source and purged with Oxygen for 30 min to remove the dissolved nitrogen gas. The anolyte was M9 salt solution with 1M glucose as the electron donor. The biocathode was E. coli cells as catalysts attached CC electrode and the anode catalysts were commercial 40％ Pt/C with a carrying capacity of 2 mg cm^{-2}. The assembled MFC voltage measurements were evaluated on a CHI 760E electrochemical workstation (Shanghai Chenhua, China). After the MFC voltage reached a steady status, the polarization and power density curves were obtained by switching the external resistors (10~300000 Ω). Besides, the output performance of MFCs under long-term operation was conducted through Keithley 2700 data acquisition system with external resistance of 2000 Ω. The MFC was operated at 37℃ and repeated for three times.

Measurement of glucose consumption level.

The glucose consumption rate of native and engineered bacteria was conducted on the conditions of battery test. The glucose concentration of different samples in MFC was detected utilizing the glucose testing kit (BC2500, Solarbio) containing reagent 1 (1 μmol/ml glucose solution) and reagent 2 and 3 (mixed in equal volume) by Cary 100 UV-VIS spectrophotometer according to the chromogenic reaction with a characteristic adsorption peak at 505 nm.

Interaction characteristic of Fe-TA complexes and Cyt c proteins

The intermolecular interactions between Fe-TA complexes and Cyt c proteins were investigated utilizing purified Cyt c as model proteins through UV/Vis absorption spectra (Cary 100 system) and Raman spectrum (LabRAM HR Evolution, Manufactred at Villeneuve d'Ascq, France). Purified horse heart Cyt c proteins (4 mg) were dissolved in 1 mL of ultrapure water, and then TA solution was added to mix well getting the Cyt c-TA sample. Similarly, Cyt c-Fe sample was obtained using ferric chloride solution. Cyt c-Fe-TA sample was obtained by adding the TA solution and ferric chloride solution successively to Cyt c solution.

DFT theoretical calculations

All DFT calculations were performed using the spin-polarized Vienna ab initio simulation package (VASP) code. The exchange-correlation functional was described by generalized gradient approximation (GGA) method in the form of Perdew-Burke-

Ernzerhof (PBE). The van der Waals (vdW) interactions were described by the DFT-D3 method. The cut-off energy was set to 500 eV and the Γ-centered Monkhorst-Pack K points of 3×3×1 and 7×7×1 was applied for geometry optimization and electronic properties. In addition, the convergence ranges for energy and force are set to 10^{-5} eV/atom and 0.01 eV/Å, respectively, throughout the calculation. Bard charges were used to analyze charge transfer in primitive reactions.

The free energy of the reaction was calculated according to the computational hydrogen electrode (CHE) model. The VASPsol code with an implicit solvation model was used to simulate the solvation effect of the electrolyte solution, and the relative permittivity of water was set to 80.76. The reaction free energy (ΔG) was calculated by this equation:

$$\Delta G = \Delta E + \Delta E_{ZEP} - T\Delta S + \Delta G_U + \Delta G_{pH} + \Delta G_{field} \quad (1)$$

where ΔE is the DFT calculated energy difference of the reaction process, ΔE_{ZEP} and $T\Delta S$ are the changes in zero-point energy and entropy between the reaction processes obtained from the vibration frequency calculation of 298.15 K. ΔG_U = eU, where U stands for the applied electrode potential, and e is the transferred charge. ΔGpH = kBT ×ln10×pH, where kB is the Boltzmann constant and pH is set to 0. ΔG_{field} is the free-energy correction, which is neglected in the present study.

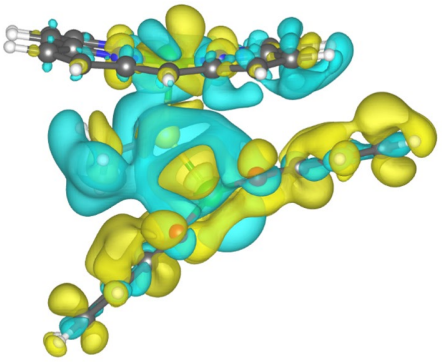

Fig. S1 The charge density differences of Cyt c-Fe-TA.

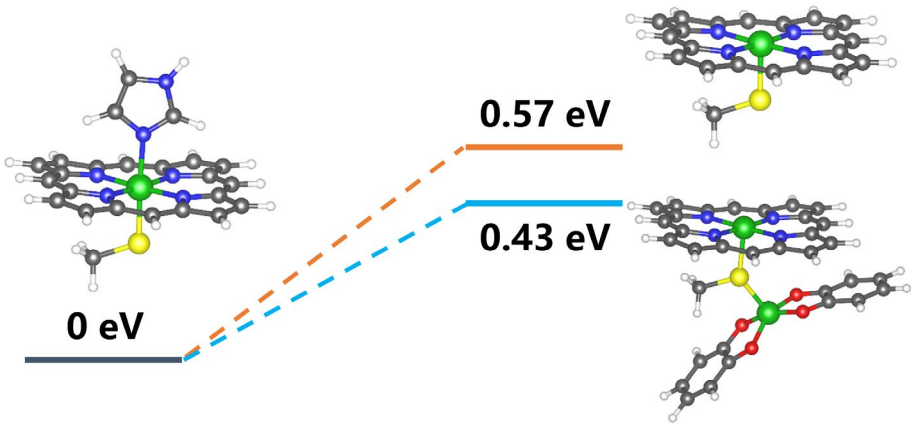

Fig. S2 Free energy diagrams of the formation of active Cyt c. The fracture of His 18 residue in native Cyt c need a free energy value of 0.57 eV, which is higher than that of Cyt c-Fe-TA (0.43 eV), showing that Fe-TA complex can reduce the energy required for Cyt c activation and stimulate Cyt c to become a catalytic five-coordination structure rapidly.

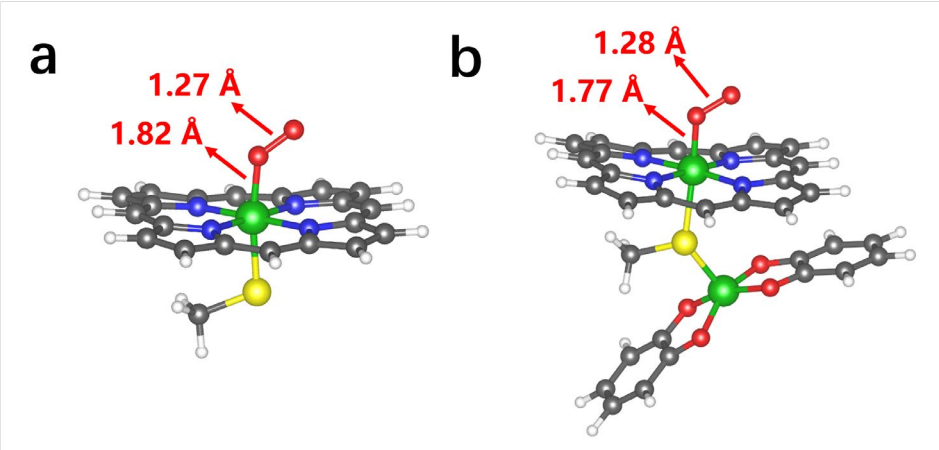

Fig. S3 The structure models of O_2 adsorption and Fe-O and O-O distances of Cyt c (a) or Cyt c-Fe-TA (b).

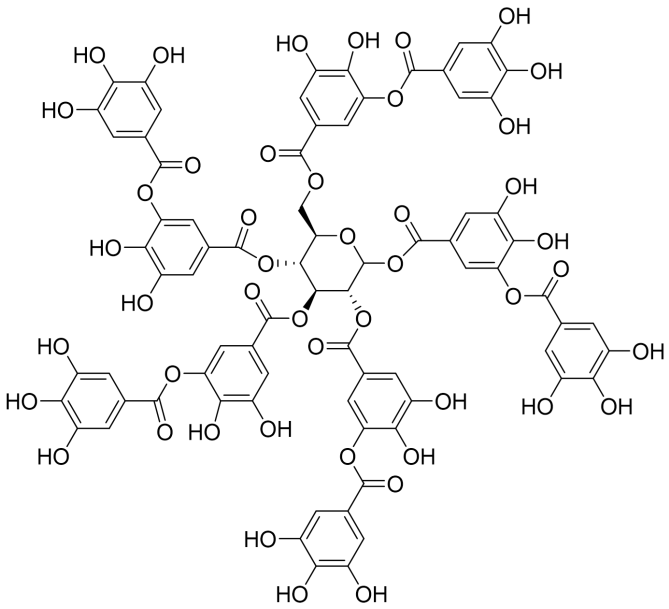

Fig. S4 The molecular structure of TA.

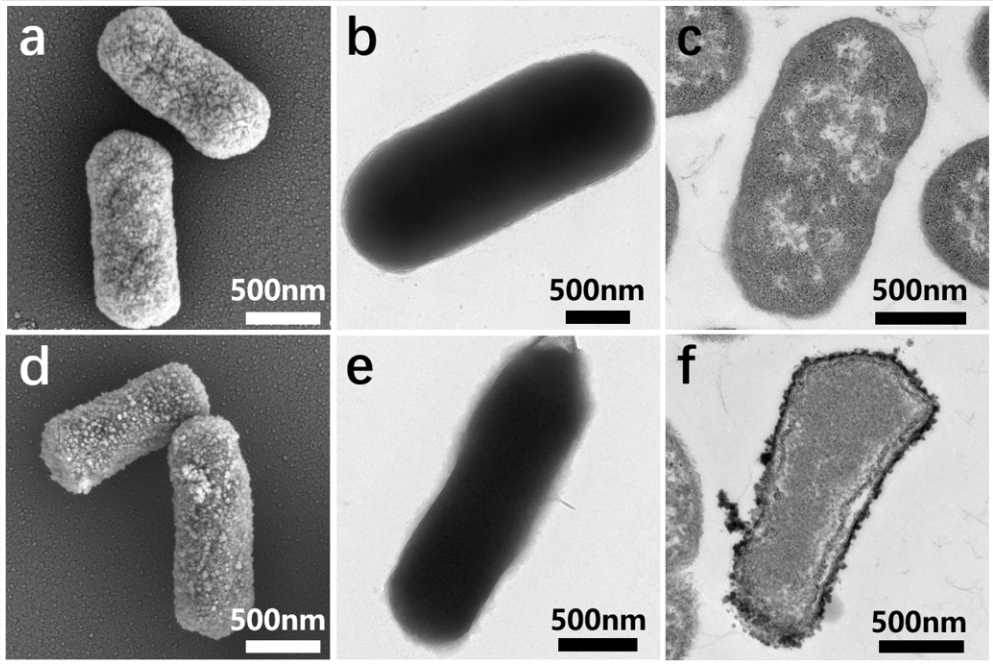

Fig. S5 (a) SEM, (b) TEM and (c) thin-section TEM images of native *E. coli* cell. (d) SEM, (e) TEM and (f) thin-section TEM images of *E. coli* cell@Fe-TA.

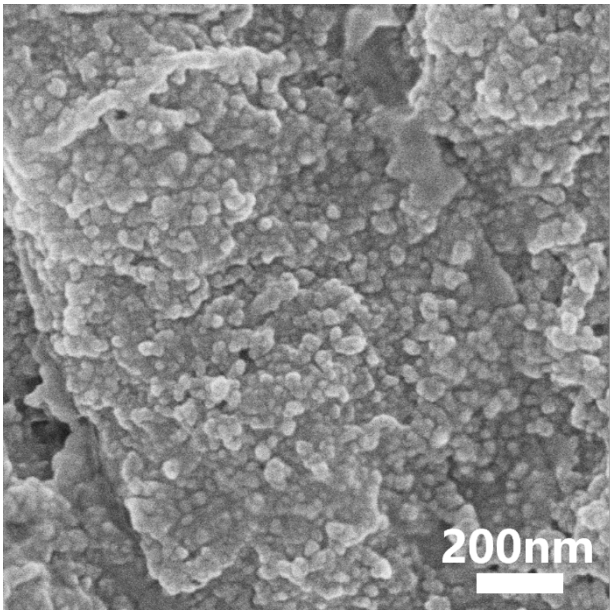

Fig. S6 SEM image of pure Fe-TA nanocomplexes.

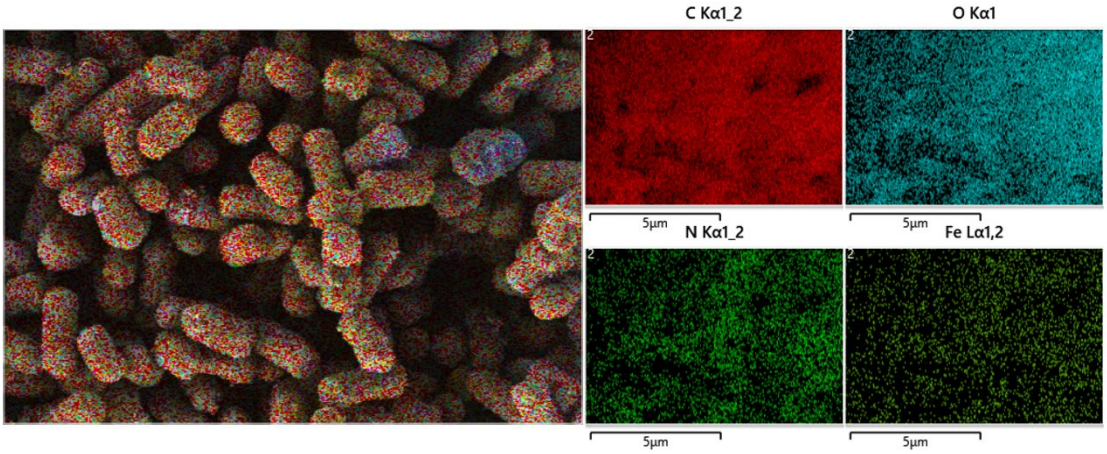

Fig. S7 SEM-EDS element mapping images of *E. coli* cell@Fe-TA.

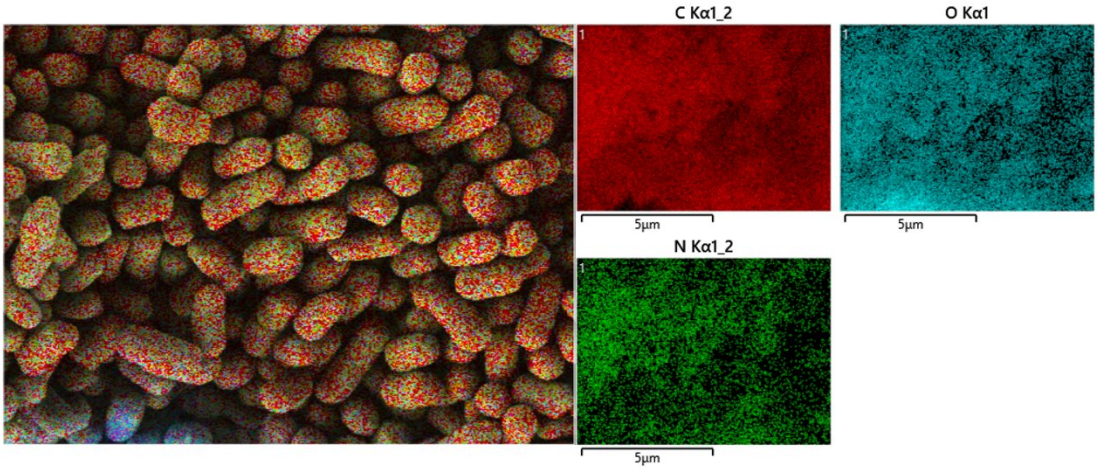

Fig. S8 SEM-EDS element mapping images of native *E. coli* cell.

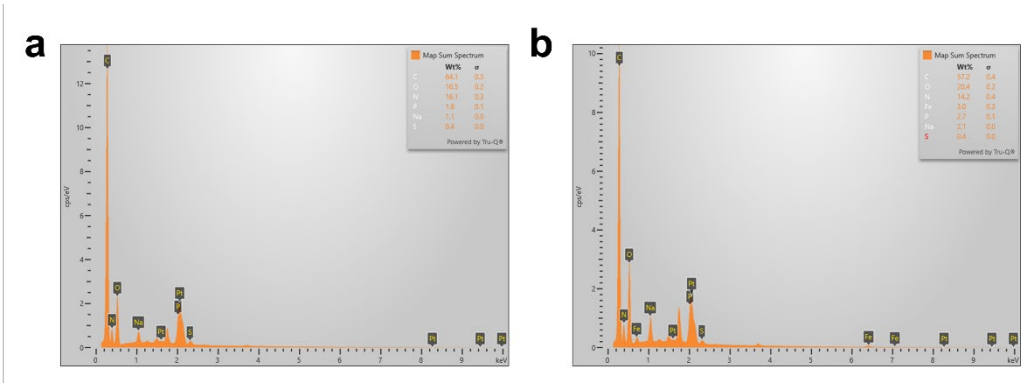

Fig. S9 SEM-EDS element content analysis of (a) native *E. coli* cell and (b) *E. coli* cell@Fe-TA.

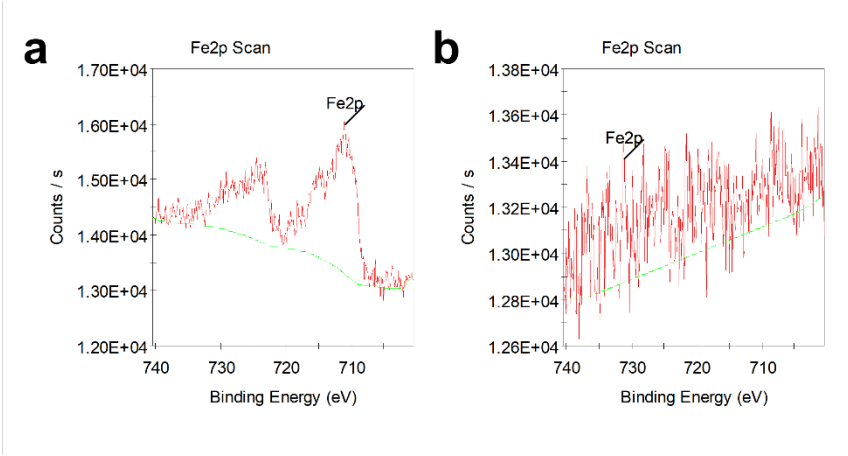

Fig. S10 Fe 2p spectrum images of XPS in (a) *E. coli* cell@Fe-TA and (b) native *E. coli* cell. *E. coli* cell@Fe-TA was detected a mass of Fe element while native *E. coli* cell was almost undetectable.

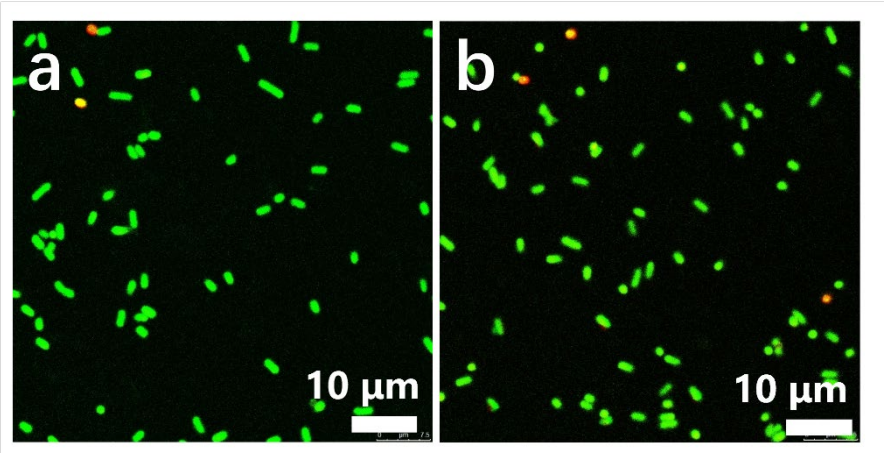

Fig. S11 The Live/Dead cell staining assay of (a) native *E. coli* cell and (b) *E. coli* cell@Fe-TA.

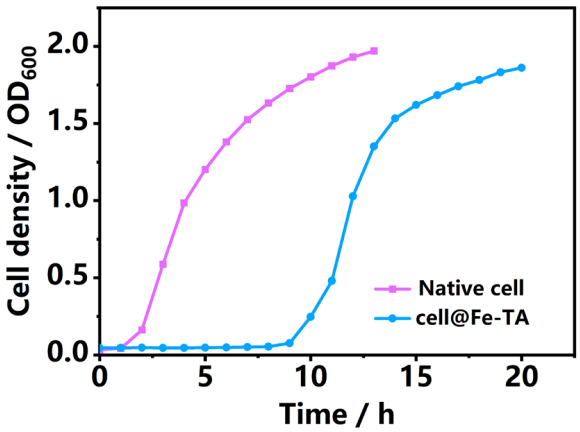

Fig. S12 Cell growth curves of native *E. coli* cell and *E. coli* cell@Fe-TA.

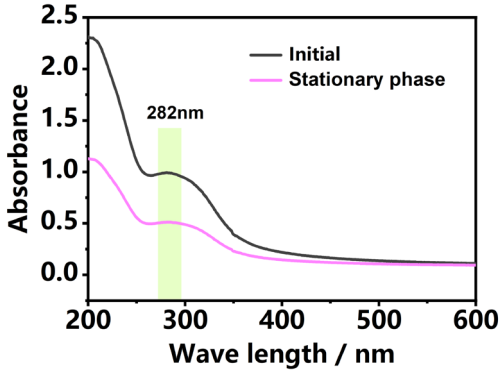

Fig. S13 UV-Visible spectroscopy test of *E. coli* cell@Fe-TA in the stationary phase of growth curve. The characteristic peak of Fe-TA is at about 282 nm.

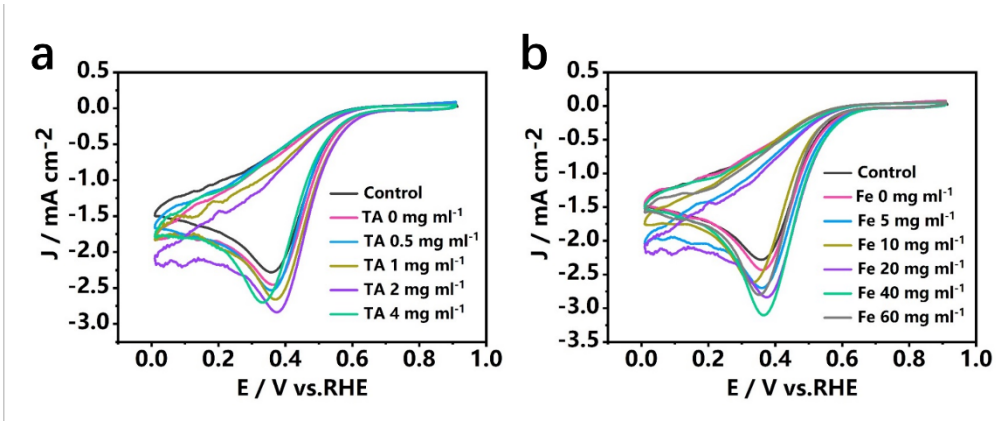

Fig. S14 Cyclic voltammetry (CV) pattern of different Fe-TA complexes concentration on *E. coli* cell (control) including (a) different TA concentration and same Fe^{3+} concentration and (b) different Fe^{3+} concentration and same TA concentration.

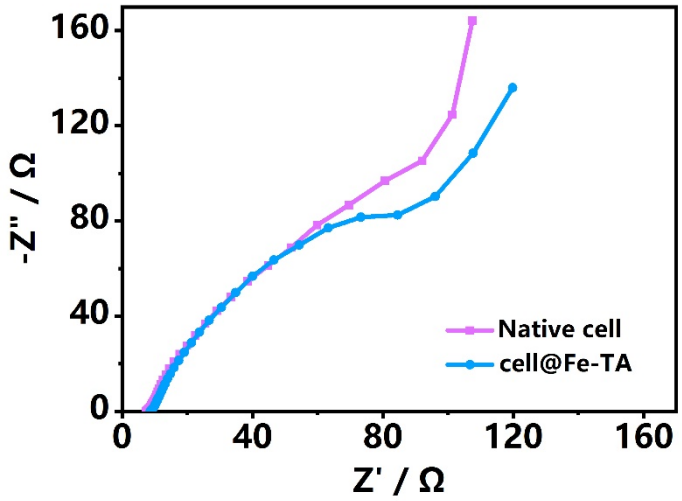

Fig. S15 Electrochemical impedance spectroscopy (EIS) plot of different cells.

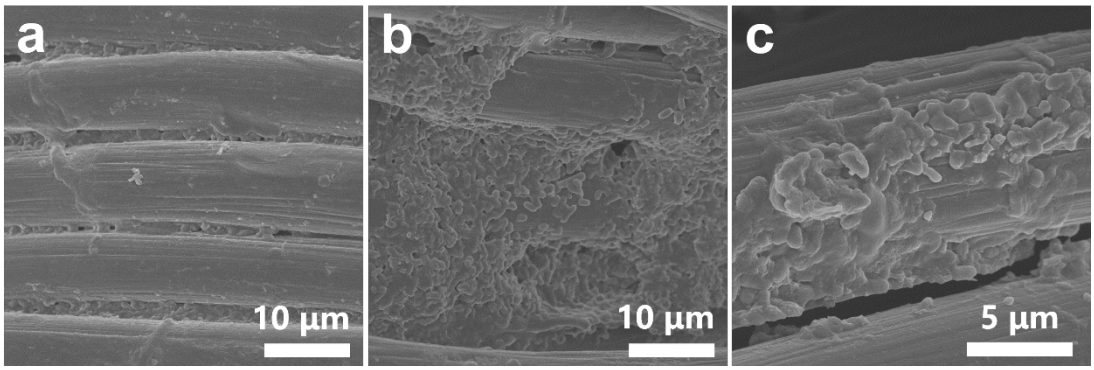

Fig. S16 FESEM images of the biofilm on the carbon cloth of (a) native *E. coli* cell and (b,c) *E. coli* cell@Fe-TA.

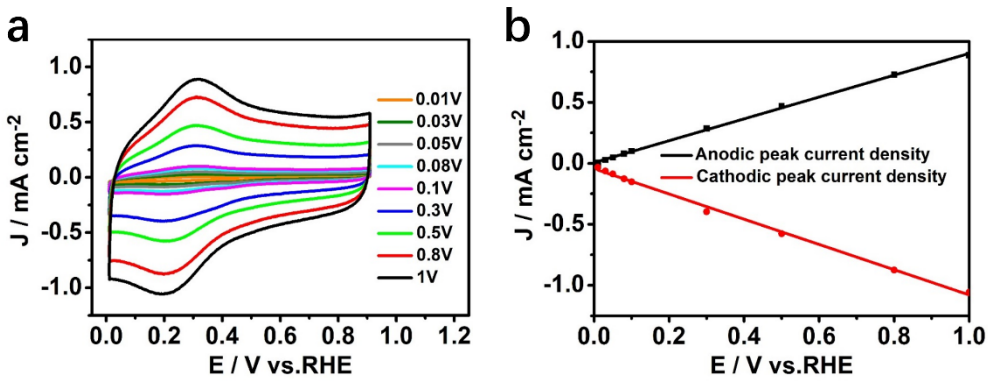

Fig. S17 (a) CVs of ET@PPy cells at 10, 30, 50, 80, 100, 300, 500, 800 and 1000 mV s^{-1}. (b) Plot of anodic peak and cathodic peak current versus scan rate.

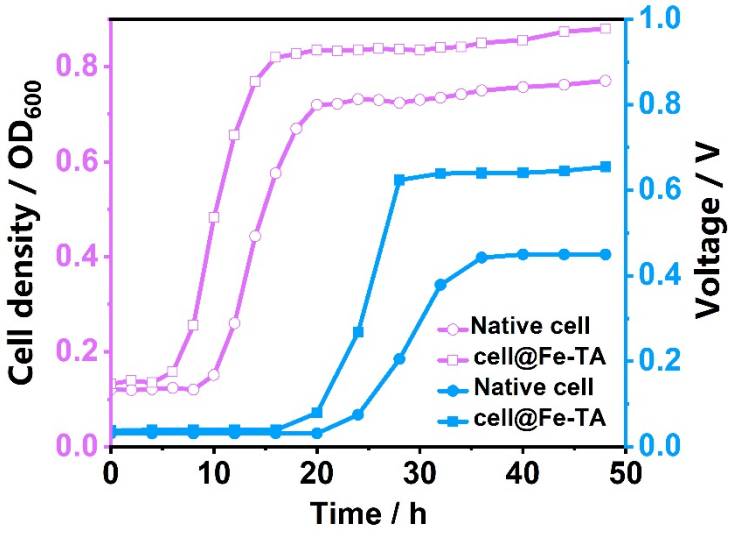

Fig. S18 Voltage output and cell growth curve at OD_{600} in MFC with different cells.

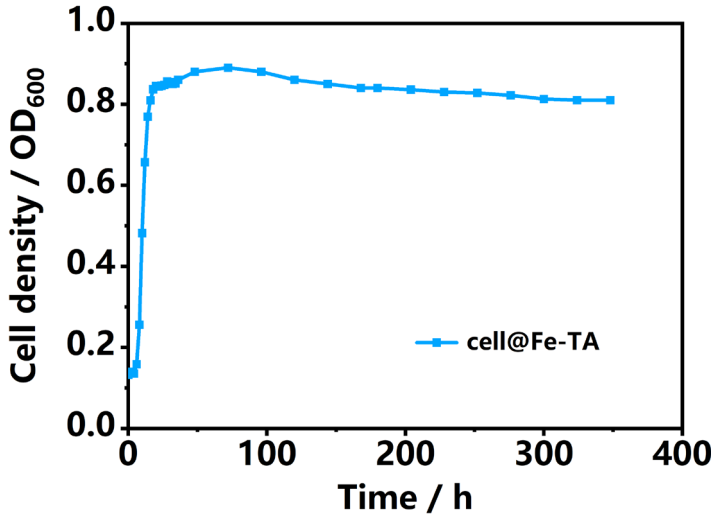

Fig. S19 Long-time growth curve of *E. coli* cell @Fe-TA in MFC test condition.

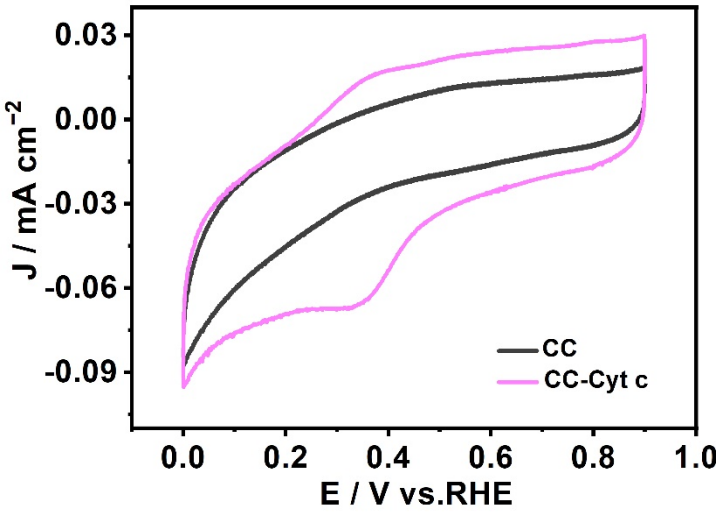

Fig. S20 Cyclic voltammetry (CV) pattern of pure Cyt c proteins in N_2 condition.

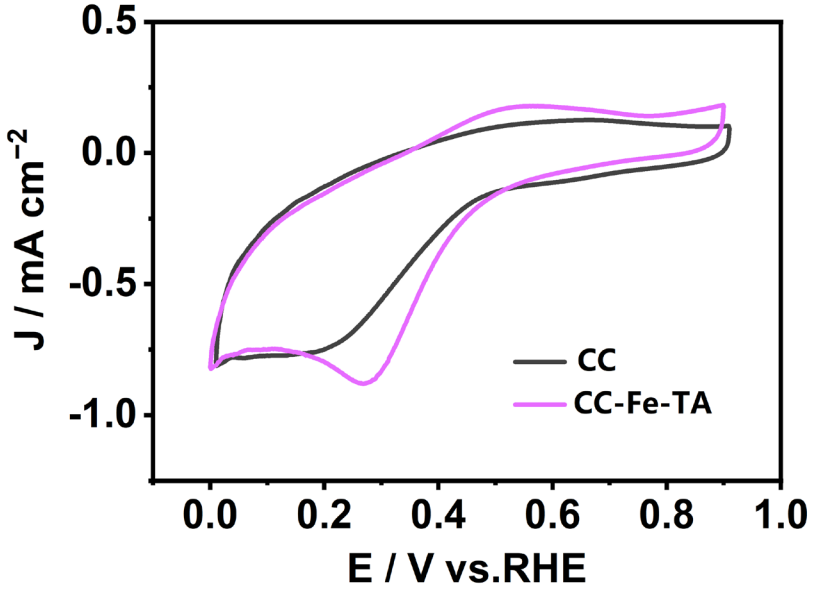

Fig. S21 Cyclic voltammetry (CV) pattern of pure Fe-TA nanocomplexes in O_2 condition.

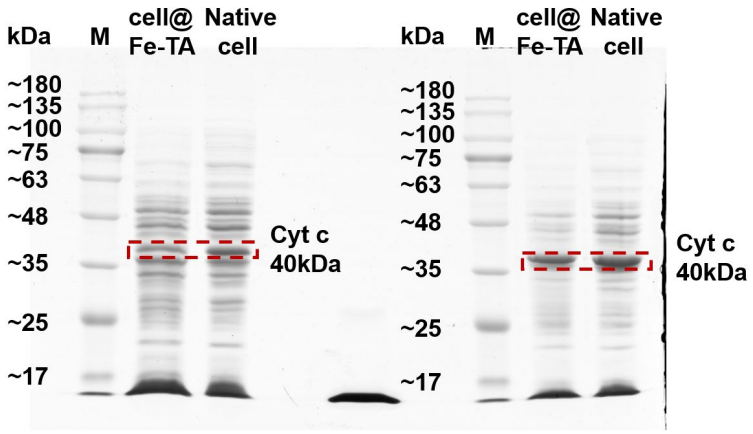

Fig. S22 The raw SDS-PAGE images of native *E. coli* cell and *E. coli* cell@Fe-TA.

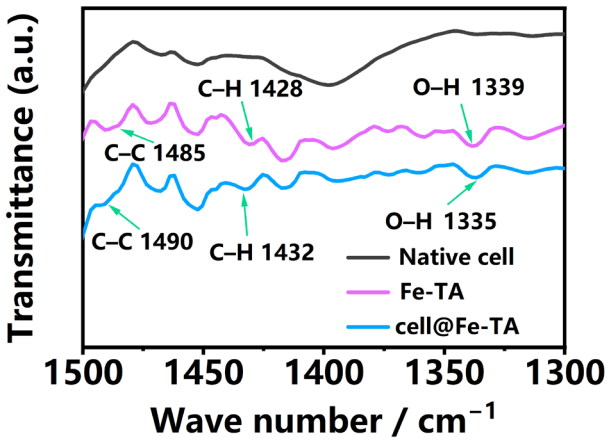

Fig. S23 FTIR spectroscopy images of native *E. coli* cell and *E. coli* cell@Fe-TA.

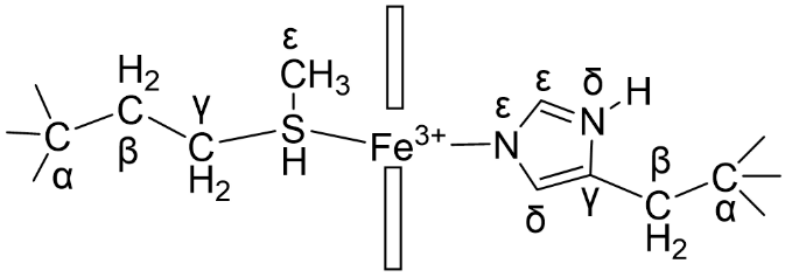

Fig. S24 The molecular structure of axial His 18 residues and Met 80 residues in Cyt c.

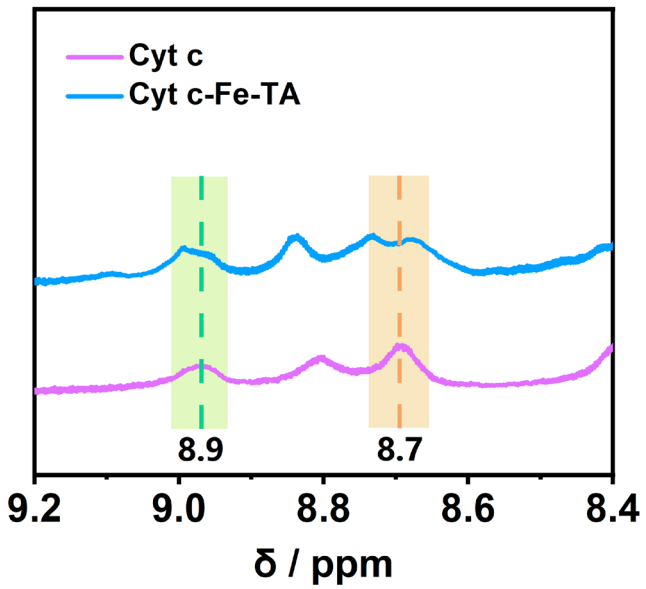

Fig. S25 Nuclear magnetic resonance (NMR) spectroscopy images of pure Cyt c proteins and Cyt c-Fe-TA complexes.

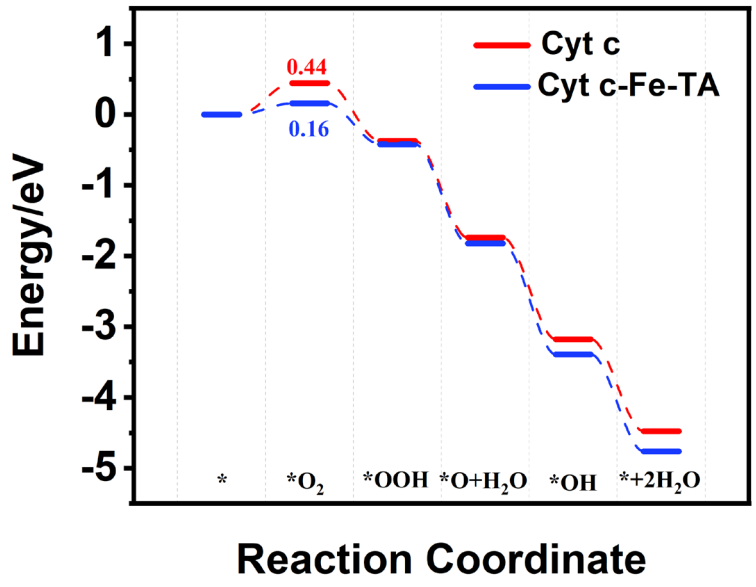

Fig. S26 Gibbs free energy diagram of ORR.

Table S1 The ORR performance comparison of other reported biocatalysts.

Catalyst	Reduction current ($mA\ cm^{-2}$)	Onset potemtial (V)	References
Hyaluronate-Au@Pt	0.17 (10 mV/s^{-1})	0.83 (vs. RHE)	ACS Appl. Energy Mater., 2022, 5: 12475-12484
Pt/C	0.16 (10 mV/s^{-1})	0.75 (vs. RHE)	ACS Appl. Energy Mater., 2022, 5: 12475-12484
Bilirubin oxidase (BOD)	0.25 (2 $mV\ s^{-1}$)	0.8 (vs. NHE)	J. Am. Chem. Soc. 2021, 143: 17236–17249
Bilirubin oxidase (BOD)	0.025 (5 $mV\ s^{-1}$)	0.55 (vs. Ag/AgCl)	Nat. Commun. 2020, 11: 316
Laccase	0.6 (1 mV/s^{-1})	0.54 (vs. Ag/AgCl)	Angew. Chem. Int. Ed. 2019, 58: 4562–4565
Engineered red blood cell	1.96 (10 mV/s^{-1})	0.53 (vs. RHE)	Angew. Chem. Int. Ed. 2019, 58: 6663–6668
Salt marsh sediments	0.28 (1 mV/s^{-1})	0.37 (vs. SCE)	Bioresource Technol. 2021, 319: 124165
***Escherichia coli*@Fe-TA**	**0.92 (1 mV/s^{-1})**	**0.66 (vs. RHE)**	**This work**

Table S2 The power generation comparison of other reported biofuel cells.

Anode catalyst	Cathode catalyst	Power density ($\mu W\ cm^{-2}$)	References
Glucose oxidase	Hyaluronate-Au@Pt	15.8	ACS Appl. Energy Mater., 2022, 5: 12475-12484
Activated sludge	Fe-NC@CBC	64.1	J. Power Sources, 2021, 512: 230522
S. oneidensis MR-1@Ag	Pt/C	660	Science, 2021, 373: 1336–1340
Yeast modified with enzymes	Laccase	36.1	J. Am. Chem. Soc., 2020, 142: 3222–3230
Pt/C	Engineered red blood cells	21.1	Angew. Chem. Int. Ed. 2019, 58: 6663–6668
Pt/C	***Escherichia coli*@Fe-TA**	**301**	**This work**

Table S3 The glucose consumption level comparison in different MFCs.

Microoganism	**Pollutant model**	**Consumption level in 100 h**	**References**
Recombinant *S. cerevisiae*-recombinant *S. oneidensis consortium*	Glucose	3.3 mM	Biochem. Eng. J. 2021, 172: 108052
Recombinant *S. cerevisiae*-recombinant *S. oneidensis consortium*	Glucose	11 mM	AIChE J. 2017, 63: 1830–1838
Gene engineered *S. oneidensis MR-1*	Glucose	12.1 mM	Bioresource Technol., 2014, 154: 59–66
Rhodoferax ferrireducens	Glucose	0.3 mM	Nat. Biotechnol., 2003, 21: 1229–1232
***Escherichia coli*@Fe-TA**	**Glucose**	**18 mM**	**This work**